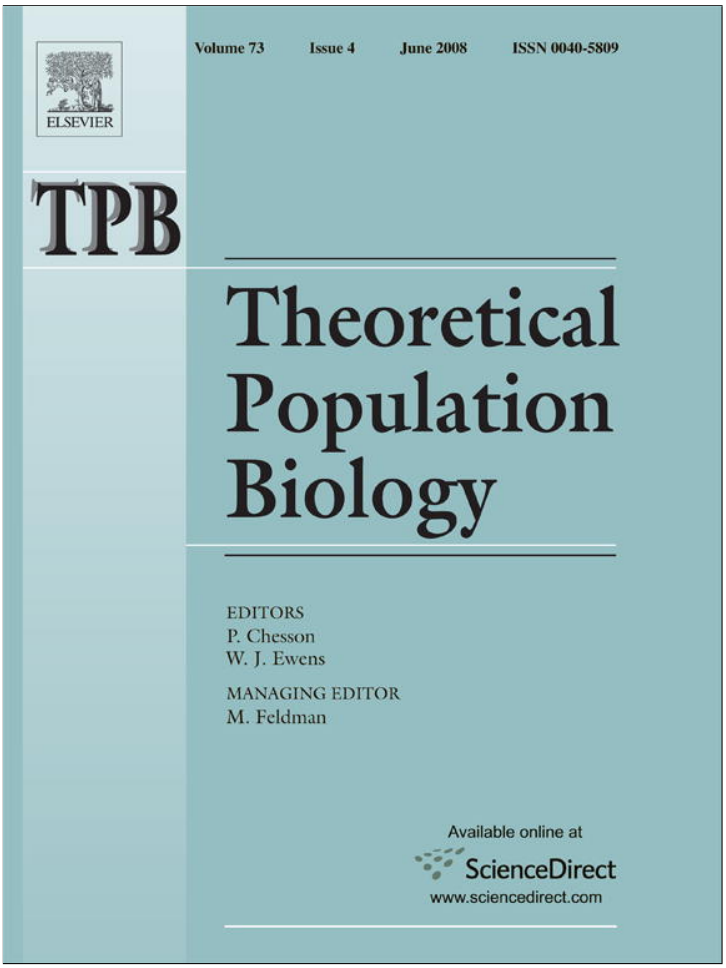

Theoretical Population Biology 73 (2008) 473–482

Contents lists available at ScienceDirect

Theoretical Population Biology

journal homepage: www.elsevier.com/locate/tpb

Population and prehistory I: Food-dependent population growth in constant environments

Charlotte T. Lee *, Shripad Tuljapurkar

Biological Sciences, Stanford University, Stanford, CA 94305, USA

ARTICLE INFO

Article history:
Received 13 June 2007
Available online 15 March 2008

Keywords:
Food limitation
Population dynamics
Dependency
Preindustrial agriculture
Resource transfers
Demographics cycles

ABSTRACT

We present a demographic model that describes the feedbacks between food supply, human mortality and fertility rates, and labor availability in expanding populations, where arable land area is not limiting. This model provides a quantitative framework to describe how environment, technology, and culture interact to influence the fates of preindustrial agricultural populations. We present equilibrium conditions and derive approximations for the equilibrium population growth rate, food availability, and other food-dependent measures of population well-being. We examine how the approximations respond to environmental changes and to human choices, and find that the impact of environmental quality depends upon whether it manifests through agricultural yield or maximum (food-independent) survival rates. Human choices can complement or offset environmental effects: greater labor investments increase both population growth and well-being, and therefore can counteract lower agricultural yield, while fertility control decreases the growth rate but can increase or decrease well-being. Finally we establish equilibrium stability criteria, and argue that the potential for loss of local stability at low population growth rates could have important consequences for populations that suffer significant environmental or demographic shocks.

1. Introduction

Population biology aims to understand the interplay between organisms and their surroundings, yet biologists have paid limited attention to the explicit study of how human populations shape and are shaped by their environment. The many fates of human societies provide abundant evidence that the environment plays a prominent role in human population dynamics. Over the sweep of history and prehistory, some societies collapsed and others thrived in ways that are or were apparently sustainable, while the ultimate fates of many are still to be determined. This paper is the first of a series that aims to provide quantitative insights into the interaction between human population dynamics and natural resource dynamics.

Our work is grounded in the study of historical processes of population change and regulation, which Lee (1986) calls "grand themes in macro-demographic theory." The aim is to formulate "a coherent theory of preindustrial population dynamics" (Wood, 1998). Lee (1986, 1987, 1993) synthesized Malthusian and Boserupian phases of population change; Wood (1998) added to this analysis a model of well-being in preindustrial societies. Anthropologists have developed theories of ecosystem–culture interactions that do not consider demography in any detail (e.g., "co-evolution" (Durham, 1976, 1991; Butzer, 1982, 1996; Kirch, 1980), and "human ecodynamics" (McGlade, 1995; van der Leeuw, 1998; van der Leeuw and McGlade, 1997; van der Leeuw and Redman, 2002)).

We follow Lee and Wood and focus on preindustrial societies, whose dynamics we expect to be closely tied to their local natural environments. The crux of our model is food, which even today remains an important link between humans and their natural environment. Shelter, disease, culture, and other factors are certainly important, but food is a major determinant of human health, mortality, and fertility, and thus of the growth rates and sizes of preindustrial agricultural populations.

We present a demographic model that describes the feedbacks between food supply and human mortality and fertility rates. We introduce parameters for the crop yield per unit area worked, the area worked per person-hour of labor, the hours worked at a given level of labor efficiency, and the labor efficiency of individuals of different ages, all assuming a particular agricultural practice and social organization of labor. These quantities and the population age structure, which determines labor supply, give the total amount of food available. We also calculate the total food needed by a population given its age structure and age-specific caloric requirements. The ratio of food available to food needed is the critical variable that determines mortality and fertility rates. There is a dynamic feedback between this *food ratio* (which

* Corresponding author.
E-mail address: charlotte.lee@stanford.edu (C.T. Lee).

0040-5809/$ – see front matter © 2008 Elsevier Inc. All rights reserved.
doi:10.1016/j.tpb.2008.03.001

depends on the population age structure) and the age structure (which depends, via mortality and fertility levels, on the food ratio). We examine the consequences of these feedbacks for the population growth rate, age structure, and measures such as life expectancy that describe well-being.

Here we consider the dynamics of expanding populations, where arable land area is not limiting. This expansion phase of population growth is relevant to the early stages of any society's adoption of agriculture, or to the success of colonization of new areas by agriculturalists (as occurred repeatedly throughout Polynesia, for example). A separate paper (Puleston and Tuljapurkar, submitted) considers the phase in population dynamics when space limits population growth. We call the dynamics of expansion "food-limited," in contrast with space-limited dynamics. Even when a population can expand in space, the rate at which it can grow and spread depends on the food gained from each unit of land. The asymptotically geometric growth in our food-limited model superficially resembles the asymptotic behavior of classical food-independent demography, but we emphasize that here, geometric growth is the outcome of fundamentally nonlinear dynamic relationships.

We show that the implications of food limitation for preindustrial human population dynamics are far-reaching. We find that the impact of environmental quality depends upon its specific demographic effects. Greater agricultural productivity decreases hunger and increases population growth and individual well-being. But favorable environments that increase survival at all hunger levels without affecting crop yield increase the growth rate but decrease well-being at equilibrium. Humans can make choices that complement or offset these environmental effects. Greater labor investments increase both population growth and well-being, and therefore can counteract lesser environmental productivity. Fertility control, on the other hand, decreases the growth rate but can either increase or decrease the well-being. The elasticities of vital rates to food are key quantities determining these and other specific effects.

This model provides a quantitative framework for examining how environment and demography interact to affect human population dynamics. Our explicit inclusion of food allows us to ask how environmental factors (such as climate and soil properties), and human factors (such as crop choice, cultivation technology and labor supply) act via food supply to affect human population dynamics, and the parameters in our model can be estimated from data. In addition, the dynamics of agricultural yield can be obtained from an agroecosystem model appropriate to a population's environment. We have developed such a model for prehistoric Hawai'i (Lee et al., 2006). Coupling the two models provides a foundation for the quantitative study of human–environment interactions in preindustrial societies, and is an important first step toward understanding why given societies developed as they did, and why some thrived while others did not.

In the next section we present the model and its novel features. The following section presents the conditions for equilibrium, when the age structure and food ratio are static while population size changes geometrically. Then we derive approximations for the population growth rate and the food ratio at equilibrium, as well as for the life expectancy and total fertility of the equilibrium population. We use the approximations to examine how the growth rate and food ratio respond to environmental variables and to human choices. In the last section we establish stability criteria for the equilibria, and show that the potential for loss of local stability at low population growth rates could have important consequences for populations that suffer significant environmental or demographic shocks. We conclude by reviewing the primary lessons of this paper and by pointing to further developments of our modeling approach.

2. The food ratio approach

We describe an age-structured population by a vector

$$\mathbf{n}(t) = N(t)\mathbf{u}(t), \tag{1}$$

with elements $n(x, t)$, the number of individuals at age x at time t. The total population size is $N(t)$, and the elements of the population age structure vector $\mathbf{u}(t)$ are $u(x, t)$, the proportion of individuals at age x at time t.

When food is plentiful enough to satisfy all nutritional requirements, fertility and survival rates are functions of age alone and are the maximal rates the population can achieve. Vital rates fall from their maxima as food consumption declines. We measure food consumption in calories relative to the consumption levels needed at each age to achieve maximal rates. The needed consumption at age x is $J\rho_x$, where J is the largest age-specific nutritional need, $\rho_x = 1$ for ages x at which consumption equals J, and $\rho_x < 1$ at all other ages. The total consumption necessary to achieve maximal rates, call it ideal consumption, is

$$J\langle \boldsymbol{\rho}, \mathbf{n}(t)\rangle = J\sum_x \rho_x n_x(t). \tag{2}$$

Assuming that area is not limiting, the supply of calories actually available per period is $YHk\langle \boldsymbol{\phi}, \mathbf{n}(t)\rangle$, where Y is the caloric yield per unit area cultivated; k is the area cultivated per person-hour of labor; H is the hours worked by the age class working the longest hours; and $\phi_x \le 1$ is the proportion of H contributed by an individual of age x.

The food ratio in a given year, $E(t)$, is the fraction of ideal consumption available:

$$E(t) = \frac{YHk}{J}\frac{\langle \boldsymbol{\phi}, \mathbf{n}(t)\rangle}{\langle \boldsymbol{\rho}, \mathbf{n}(t)\rangle} = \frac{YHk}{J}\frac{N\langle \boldsymbol{\phi}, \mathbf{u}(t)\rangle}{N\langle \boldsymbol{\rho}, \mathbf{u}(t)\rangle} = \frac{YHk}{J}\frac{\langle \boldsymbol{\phi}, \mathbf{u}(t)\rangle}{\langle \boldsymbol{\rho}, \mathbf{u}(t)\rangle}. \tag{3}$$

When $E < 1$, the population is food-limited, and vital rates are less than maximal. At $E \ge 1$, vital rates are maximal.

In Eq. (3), food production and food demand scale linearly with population size N; if the population were limited by space, food production would decrease with increasing N (Puleston and Tuljapurkar, submitted). As an index of production relative to consumption, the food ratio E is the inverse of a weighted dependency ratio (demographic dependency ratios are discussed, e.g., by Lee (1994)). Food is thus transferred between workers and non-workers (e.g., from adults to children); Lee (2003) explores the evolutionary implications of such transfers. Sharing food on the basis of need is one possible allocation scheme (a "big-pot" method of sharing; see Gurven 2003 for a review of the empirical literature), and Eq. (3) could be modified to accommodate others. For instance, one could allot a fraction η_x of E to age group x in order to explore different strategies $\boldsymbol{\eta}$, and possibly to identify an optimal strategy (see, e.g., Chu and Lee (2006)). Here we focus on Eq. (3) as a starting point.

At age x, the one-year survival rate is p_x, survivorship is l_x, and fertility is m_x. Each of these depends on the food ratio $E(t)$, and we find it convenient to consider them as functions of $\log E(t)$. We assume that at the maximum survival and fertility rates, $p_x(\log E = 0)$ and $m_x(\log E = 0)$, the population has a positive asymptotic growth rate, and that $p_x(\log E)$ and $m_x(\log E)$ are monotonic increasing functions of E. These functions encapsulate the biological response of the population to food availability. The elasticities of survival and fertility at age x with respect to E are α_x and γ_x:

$$\frac{dp_x}{d\log E} = \alpha_x p_x, \quad \frac{dm_x}{d\log E} = \gamma_x m_x. \tag{4}$$

Survivorship $l_x = p_1 p_2 \cdots p_{x-1}$, so the elasticity of l_x is

$$\frac{d\log l_x}{d\log E} = \beta_x = \sum_{y=1}^{y=x-1} \alpha_y, \tag{5}$$

Table 1
Examples of model parameters affected (*) by environmental and human factors

Parameter Interpretation	Y Yield/area	H Max. hours	k Area/hour	ϕ_x Prop. of H at age x	$m_x(0)$ Max. fertility	$p_x(0)$ Max. survival	α_x Surv. elasticity	γ_x Fert. elasticity
Soil fertility	*							
Climate	*	*	*		*	*	*	*
Crop choice	*							
Agricultural technique	*	*	*	*				
Cultural preferences		*		*	*	*		*

and β_x is an increasing function of age.

The parameters in our model subsume a good deal of detail about the environment and society. A given physical, biological, cultural, and technological milieu implies particular values for the yield per unit area, Y, the characteristic hours worked by an efficient individual, H, the corresponding land area worked, k, and the hours contributed at different ages, ϕ_x, but different parameter choices can accommodate other settings. For instance, an age pattern of work ϕ_x will characterize sweet potato cultivation on leeward volcanic slopes in Hawai'i, but many individuals in such a population who do not usually work (e.g., the relatively young) might be capable of contributing some labor. Flexibility in the age pattern of contributions to the labor force depends upon the priorities and organization of the population, and can be captured by varying ϕ_x. Similarly, the yield parameter Y depends on cultivation techniques and environmental quality, e.g. rainfall and soil fertility. We can represent changes in these factors (such as the adoption of mulching in addition to all other practices, which would require more labor and might reduce the land area worked, but could also raise yields), by changing model parameters. Table 1 indicates which parameters would most likely change in response to shifts in a number of important environmental and cultural factors.

Demographic parameters likewise respond to environmental and social influence, and may vary between populations as a result. Maximal survival rates $p_x(0)$ respond to environmental factors such as winter temperatures and disease prevalence. In addition, they depend on cultural, social, and technological factors such as the practice of infanticide or geronticide and the frequency of warfare. Maximal fertility $m_x(0)$ also has both human and environmental components, but human factors may play a comparatively larger role because fertility responds to individual choices as well as to social norms. Survival elasticities α_x describe physiological responses to food shortages. Although measured responses of survival to food may have social dimensions, differences between social classes are frequently due to inequality in access to food during times of hardship (Bengtsson et al., 2004). Our model assumes that food shortages are experienced equally by all individuals, and in effect averages over any underlying social or other inequalities; modification of the model could enable us to address these issues. Finally, physiology plays an important role in determining fertility elasticities γ_x; but as in the case of maximal rates, fertility elasticities are more likely to depend on human decisions than do survival elasticities. For instance, in times of food shortage, humans may reduce fertility by delaying marriage or by increasing migration of one sex, usually males, which may separate couples; these actions would be reflected in the elasticity of fertility rates (Bengtsson et al., 2004). Table 1 shows how demographic model parameters may respond to environmental and human factors. Our food ratio approach thus enables us to explore the quantitative implications of specific scenarios, such as the colonization of a new region with a given cultivation technology, or the practice of different forms of fertility control.

3. Dynamics and equilibrium

The population's dynamics follow the matrix equation

$$\mathbf{n}(t+1) = \mathbf{A}(t)\mathbf{n}(t), \tag{6}$$

where the nonzero elements of the projection matrix $\mathbf{A}(t)$ are $A(t, 1, x) = m_x(E(t))$ and $A(t, x+1, x) = p_x(E(t))$, and $E(t)$ is computed from Eq. (3).

At equilibrium the food ratio is constant, $E(t) = \hat{E}$, and

$$\mathbf{n}(t+1) = \mathbf{A}(\hat{E})\mathbf{n}(t) = \hat{\lambda}_1\mathbf{n}(t). \tag{7}$$

Hence at equilibrium, $\mathbf{n}(t)$ is proportional to $\hat{\mathbf{u}}_\mathbf{1}$, the right eigenvector of the equilibrium projection matrix $\mathbf{A}(\hat{E})$ corresponding to its dominant eigenvalue, $\hat{\lambda}_1$. This eigenvalue is determined by the characteristic equation

$$\sum_x l_x(\hat{E})m_x(\hat{E})\hat{\lambda}_1^{-x} = 1. \tag{8}$$

If the equilibrium is stable, then starting from any initial condition, the population eventually grows at the geometric rate $\hat{\lambda}_1$ and has a stable age structure $\hat{\mathbf{u}}_\mathbf{1}$. Additionally, because we assume that the land area cultivated per person-hour is constant, $\hat{\lambda}_1$ also measures the population's rate of spatial expansion.

The equilibrium age structure is related to equilibrium growth rate and survivorship by

$$\hat{u}_1(x) = cl_x(\hat{E})\hat{\lambda}_1^{(-x+1)}, \tag{9}$$

where the constant c is chosen so that $|\hat{\mathbf{u}}_\mathbf{1}| = \sum_x \hat{u}_1(x) = 1$. The equilibrium food ratio is

$$\hat{E} = \frac{YHk}{J}\frac{\langle\boldsymbol{\phi}, \hat{\mathbf{u}}_\mathbf{1}\rangle}{\langle\boldsymbol{\rho}, \hat{\mathbf{u}}_\mathbf{1}\rangle} = \frac{YHk}{J}\frac{\sum_x \phi_x l_x(\hat{E})\hat{\lambda}_1^{-x}}{\sum_x \rho_x l_x(\hat{E})\hat{\lambda}_1^{-x}}. \tag{10}$$

Eqs. (8) and (10) simultaneously determine the equilibrium values $\hat{\lambda}_1$ and $\hat{E}$. Eq. (8) yields a positively sloped curve of E versus λ_1, since higher growth rates are associated with higher vital rates. Eq. (10) describes the feedback between production and consumption. For a fixed E, the fraction of working individuals is small when λ_1 is small and the age structure is skewed to old ages, and also small when λ_1 is large and the age structure is skewed to young ages. Thus in general for a given E there are two values of λ_1 that satisfy (10), and thus two curves relating E and λ_1. Only one of these intersects with the solution curve of (8) to determine $\hat{E}$ and $\hat{\lambda}_1$. Fig. 1 presents equilibrium condition (8) (lines without symbols) and the relevant curve for condition (10) (lines with symbols) graphically in (λ_1, E) space, with equilibrium occurring at their intersection.

The solutions of Eq. (8) depend only on mortality, fertility, and their elasticities, while solutions of Eq. (10) are not affected by fertility rates but do depend on all other model parameters. Fig. 1 illustrates these dependencies. The left-hand panel shows the equilibria for two values of yield, Y. The solution curve of Eq. (8) (solid line without symbols) is unaffected by the change in Y. The two curves with symbols show the solution curves of Eq.

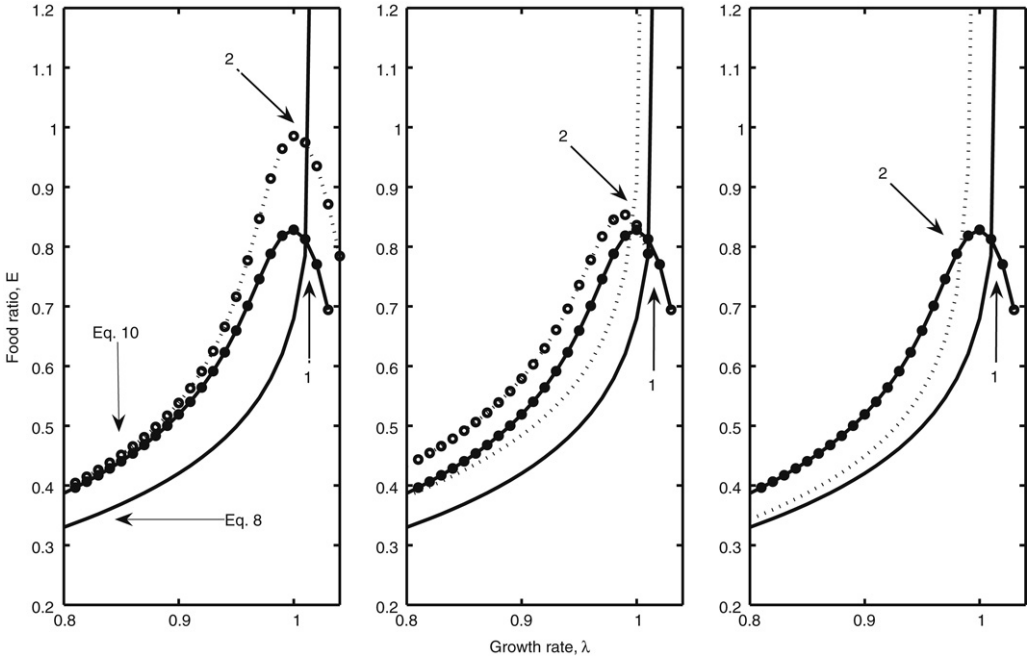

Fig. 1. Effects of parameter changes on equilibrium conditions (8) (lines without symbols) and (10) (lines with symbols). Left panel: increasing agricultural yield Y or lengthening the work schedule ϕ_x shifts solutions of (10) up (dotted line with symbols), shifting the equilibrium point from 1 to 2. Center panel: changing baseline survival rates $l_x(0)$ or survival elasticities $\alpha_x(0)$ shifts both conditions (dotted lines). Right panel: changing baseline fertility rates $m_x(0)$ or fertility elasticities $\gamma_x(0)$ shifts condition (8) only (dotted line).

(10) for the two different yields. With all else being equal, higher yields (such as might occur with higher levels of rainfall) shift the equilibrium from the intersection marked with a numeral 1 to the equilibrium marked 2, resulting in faster population growth and spatial spread (higher $\hat{\lambda}_1$) and greater food consumption (higher $\hat{E}$). Lengthening the work schedule by recruiting younger and older individuals to agricultural labor has the same effect: the curve for Eq. (8) is unaffected while the curve for Eq. (10) shifts up, increasing both $\hat{E}$ and $\hat{\lambda}_1$. In general, changes in model parameters that affect only condition (10) shift the equilibrium food ratio and growth rate in tandem.

The center panel of Fig. 1 illustrates the effects of parameter changes that affect both equilibrium conditions. Examples of such changes include decreases in maximal survival rates or increases in survival elasticities, which could be caused by less favorable climate. In response both curves shift up, resulting in a higher equilibrium food ratio but a lower population growth rate. Conversely, increasing the maximal survival rates or decreasing the survival elasticities shifts both curves down. In general, parameter changes that shift both curves may or may not have conflicting effects on $\hat{E}$ and $\hat{\lambda}_1$. The right-hand panel illustrates the effect of shifting only solutions to Eq. (8). Lowering maximal fertility rates or increasing fertility elasticities, changes that correspond to across-the-board fertility control or control only when food is scarce, both shift the curve of Eq. (8) up. The net result in Fig. 1 is a lower growth rate and a food ratio that is nearly unchanged. In general, parameter changes that affect only Eq. (8) have predictable effects on $\hat{\lambda}_1$, but the effect on $\hat{E}$ depends on the shape of the curve (10) and the magnitude of the parameter change.

3.1. Approximate expressions for equilibrium quantities

It is clear from the preceding graphical analyses that trade-offs exist between environmental and human dimensions of food-limited demography. Human decisions regarding labor organization and fertility control may work in tandem with or in opposition to changes in environmental conditions, such as shifts in productivity or in maximal survival rates. To quantify the effects of different forces on equilibrium, we now develop approximations for the population growth rate, the food ratio, life expectancy at birth, and total fertility rate. The approximations are based on Taylor expansions of the two nonlinear equilibrium conditions around the point ($\log E = 0$) where the population achieves its maximal growth rate ($\lambda_1(0)$).

We use (3) to define the yield, $Y(0)$, needed to achieve the food ratio $\log E = 0$. To achieve $E = 1$ requires a yield

$$Y = Y(0) = \frac{J}{Hk}\frac{\langle \boldsymbol{\rho}, \mathbf{u_1}(0)\rangle}{\langle \boldsymbol{\phi}, \mathbf{u_1}(0)\rangle}. \tag{11}$$

Yields equal to or greater than $Y(0)$ result in the best of possible worlds, where food supply is sufficient to achieve maximal vital rates and population growth. The right-hand side of the equation emphasizes that $Y(0)$ depends on the population's maximal vital rates, age-specific labor contributions and calorie requirements, environment, agricultural technology, and culture (see Table 1). At equilibrium with $Y < Y(0)$, growth rate $\hat{\lambda}_1 < \lambda_1(0)$, and food ratio $\log \hat{E} < 0$, we find (see Appendix A) that $\hat{E}$ is related to the scaled yield $Y/Y(0)$ by

$$\hat{E} \approx \left(\frac{Y}{Y(0)}\right)^{K_1}, \tag{12}$$

and the scaled growth rate $\hat{\lambda}_1/\lambda_1(0)$ is related to $\hat{E}$ by

$$\frac{\hat{\lambda}_1}{\lambda_1(0)} \approx \hat{E}^{K_2}. \tag{13}$$

The quantity K_1 is a positive but complicated function of many parameters of the maximally growing population (Appendix A). Fortunately, numerical analysis reveals that $K_1 \approx 1$ for a wide range of reasonable parameter choices (see Appendix B), so that roughly speaking, $\hat{E} \approx Y/Y(0)$. This is intuitively appealing: if the yield is half what is needed to achieve the best possible world, then at equilibrium, the food available is also roughly half what

is needed. One might predict this outcome from naive arguments concerning agricultural yield, without considering nonlinearities in population demography. Combining (11) and (12) with $K_1 \approx 1$, we obtain

$$\hat{E} \approx \frac{YHk}{J} \frac{\langle \boldsymbol{\phi}, \mathbf{u_1(0)} \rangle}{\langle \boldsymbol{\rho}, \mathbf{u_1(0)} \rangle} \tag{14}$$

which transparently relates the equilibrium food ratio to yield, labor schedule, calorie requirements, and maximum survival and fertility rates. In the next section we examine in more detail the effects on $\hat{E}$ of changes in individual environmental and human parameters.

K_2 in Eq. (13) is equal to ν_G/T_G, where ν_G is a weighted average of the survival and fertility elasticities at $\log E = 0$, and T_G is the generation time at maximal survival and fertility (details in Appendix A). K_2 is independent of production and consumption schedules, and although it varies with maximal rates and their elasticities, it is always positive and on the order of 10^{-2}. Therefore $\hat{\lambda}_1/\lambda_1(0)$ is an increasing concave function of $\hat{E}$ (conversely, $\hat{E}$ is a convex increasing function of $\hat{\lambda}_1$, corresponding to the lines without symbols in Fig. 1). We can write this nonlinear relationship in the form

$$\hat{\lambda}_1 \approx \lambda_1(0) \left[\hat{E}^{\nu_G}\right]^{1/T_G}, \tag{15}$$

which is a food-dependent counterpart to the classic demographic result (Keyfitz, 1968) that the growth rate scales as the net reproductive rate (NRR) raised to the inverse of the generation time. Here the NRR scales as $\hat{E}^{\nu_G}$. This intuitively reasonable result indicates that the vital rates that determine NRR are concave increasing functions of the food ratio, with the degree of nonlinearity determined by the elasticities of the rates to food. We discuss below in more detail how parameter changes affect the growth rate; here we note that numerically, we find that increasing maximal survival rates decreases K_2, all else being equal, while increasing maximum fertility increases K_2.

We can expand the terms in the expression for life expectancy at birth to obtain the approximation

$$\hat{e}_0 \approx \sum_x \hat{l}_x \approx e_0(0) + \log \hat{E}^{\langle \boldsymbol{\beta}(\mathbf{0}), \mathbf{l}(\mathbf{0}) \rangle} \tag{16}$$

and similarly expand the total fertility rate (TFR),

$$\widehat{\mathrm{TFR}} = \sum_x \hat{m}_x \approx \mathrm{TFR}(0) + \log \hat{E}^{\langle \boldsymbol{\gamma}(0), \mathbf{m}(0) \rangle}, \tag{17}$$

where $e_0(0)$ and TFR(0) are the maximal life expectancy and maximal TFR, hats indicate equilibrium values, $\boldsymbol{\beta}(0)$ and $\boldsymbol{\gamma}(0)$ are vectors of the elasticities of survivorship and fertility evaluated at $\log E = 0$, respectively, and $\mathbf{l}(0)$ and $\mathbf{m}(0)$ are vectors of maximal survivorship and fertility. The relationships (16) and (17) translate relative food deprivation into its concrete, biological consequences. Together with $\hat{\lambda}_1$, which measures population growth and spatial expansion, and the food ratio $\hat{E}$, which describes the extent to which individuals' needs are met, the equilibrium life expectancy and total fertility rate provide means to assess average well-being in food-limited populations.

For a wide range of plausible parameter values (see Appendix B), $\langle \boldsymbol{\beta}(0), \mathbf{l}(0) \rangle$ varies between approximately 10 and 25, while $\langle \boldsymbol{\gamma}(0), \mathbf{m}(0) \rangle$ varies between about 0.2 and about 0.7. Table 2 gives a few examples of the resulting range of effects on equilibrium life expectancy and TFR as a function of $\hat{E}$. In some cases the response is substantial; we discuss responses to specific parameter changes in more detail in the next section.

By making some stylized assumptions, we can simplify (12) and (13) . Approximate the age pattern of survival elasticities α_x using a constant value α, and fertility elasticities γ_x by γ. Then

Table 2
Range of percentage reductions from maximum in life expectancy (e_0) and total fertility rate (TFR) at decreasing equilibrium food ratios

$\hat{E}$	% change in e_0	% change in TFR
1	0	0
0.8	[3.0, 18.6]	[1.5, 2.9]
0.6	[6.9, 42.6]	[3.4, 6.7]

$\beta_x = \alpha x$. Further, we can usefully approximate the age schedules of production and consumption by constant levels $\phi_x = \phi$ for $x \geq 15$ and $\rho_x = \rho$ for all x. Using these stylized schedules, we find (Appendix A) that

$$\left(\hat{\lambda}_1/\lambda_1(0)\right) \approx (Y/Y(0))^{\alpha[1-2\alpha(T_\phi - T_\rho)]}, \tag{18}$$

where T_ϕ and T_ρ are the population average ages of production and consumption, respectively. We can easily see that an increase in α increases the exponent (when $\alpha < 1/[2(T_\phi - T_\rho)]$) and so decreases $\hat{\lambda}_1$. In addition, the response of life expectancy and TFR to the equilibrium food ratio simplifies in an interesting way:

$$\hat{e}_0 \approx e_0(0) + \frac{\alpha\,(e_0^2 + S_0^2)}{2} \log \hat{E},$$

and

$$\widehat{\mathrm{TFR}} \approx \mathrm{TFR}(0)\left(1 + \gamma \log \hat{E}\right).$$

Here S_0^2 is the variance in the age at death (for the derivation of this result, see Appendix C). The first equation above shows that, all else being equal, the decline in $\hat{e}_0$ when the food ratio declines is larger in populations with a high $e_0(0)$ and in populations with a higher variance in age at death. A high variance occurs in populations with high infant and child mortality and relatively even adult mortality (Edwards and Tuljapurkar, 2005). The response of TFR is simpler: the elasticity of TFR is simply γ.

3.2. Environmental and human contributions to equilibrium quantities

We now investigate the quantitative effects of specific parameter changes on the equilibrium growth rate, food ratio, life expectancy, and total fertility rate. We illustrate relationships (12) and (13) in Fig. 2 using parameters appropriate to preindustrial Polynesian societies (see Appendix B for details). We construct two scenarios that span the range of conditions that typical populations are likely to have encountered. One is a favorable case (solid lines), where all parameters encourage fast population growth at equilibrium: maximum life expectancy and maximum fertility are high, all elasticities are low, and labor schedules are long. In the unfavorable scenario (dashed lines), all parameters bias the population toward low growth rates. We use these scenarios to provide concrete, graphical illustrations of the effects of parameter changes as an alternative to calculating derivatives (e.g., Caswell (2008)). The left panel of Fig. 2 shows $\hat{\lambda}_1/\lambda_1(0)$ as a function of $\hat{E}$ (or of $Y/Y(0)$). The unfavorable scenario results in lower equilibrium growth rates for a given value of $\hat{E}$ than the favorable scenario. Scaling Y by $Y(0)$ and $\hat{\lambda}_1$ by $\lambda_1(0)$, however, obscures some of the effects of demographic changes because the scaling quantities themselves differ between the two cases. The center panel of Fig. 2 shows $\hat{E}$ and the right panel shows $\hat{\lambda}_1$ as functions of Y in units of tons of crop per hectare. The unfavorable scenario lowers $\hat{E}$ for a given value of Y versus the favorable scenario because $Y(0)$ is higher, as we explain in more detail below. In the right-hand plot, $\hat{\lambda}_1$ as a function of Y is affected by this difference in $\hat{E}$ and differences in $\lambda_1(0)$ in addition to the changes in Eq. (13) shown in the left panel.

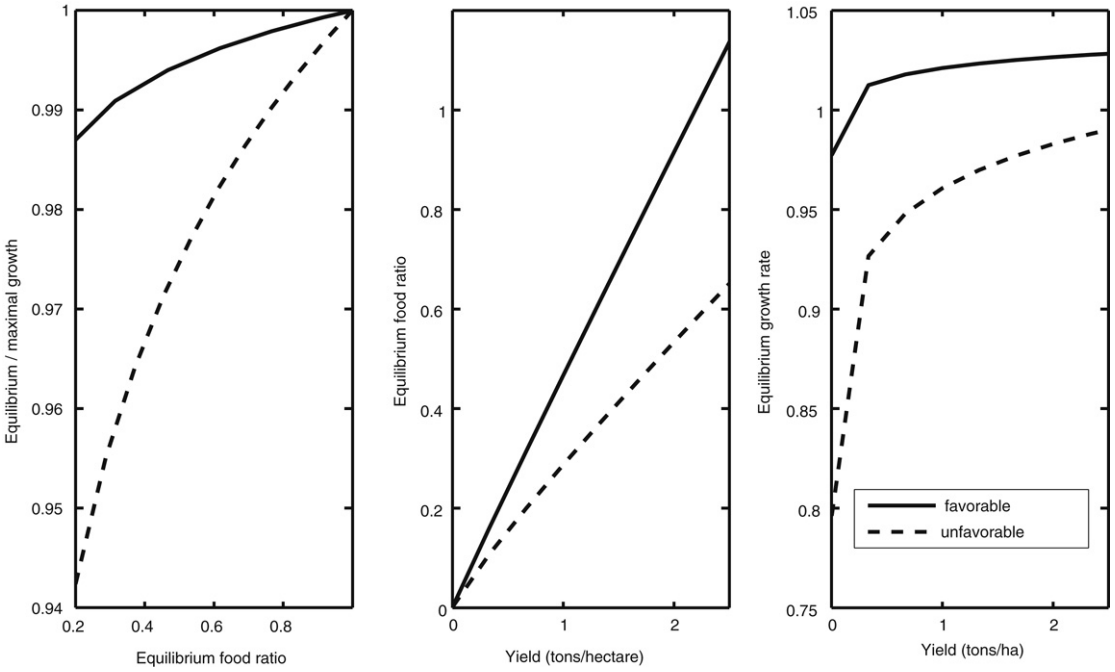

Fig. 2. Relationships between equilibrium growth rate, food ratio, and yield under favorable (solid lines) and unfavorable conditions (dashed lines). Left panel: the relative equilibrium growth rate $\hat{\lambda}_1/\lambda_1(0)$ falls faster with decreasing equilibrium food ratio $\hat{E}$ under unfavorable conditions. Center panel: the equilibrium food ratio as a function of yield increases less quickly under unfavorable conditions. Right panel: the two effects combine in $\hat{\lambda}_1$ as a function of yield. Favorable: all parameters bias the population toward fast growth. Unfavorable: all parameters bias toward slow growth.

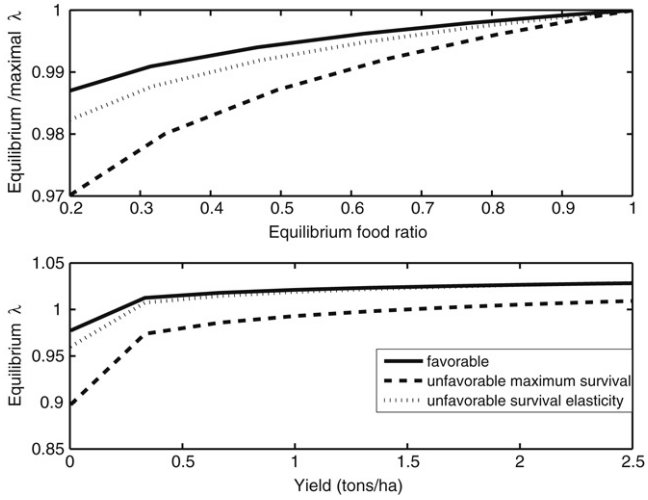

Fig. 3. Relationships between equilibrium growth rate, food ratio, and yield as a function of survival conditions. Top panel: halving $e_0(0)$ (dashed line) or doubling $\alpha_x(0)$ (dotted line) decreases relative equilibrium growth rate as a function of $\hat{E}$ compared to all favorable conditions (solid line). Bottom panel: effects on unscaled equilibrium growth rate as a function of yield.

Having constrained the reasonable range of responses of $\hat{E}$ and $\hat{\lambda}_1$ by shifting suites of parameters, we now consider the effects of individual parameter changes. First, consider the effects of changing between long and short work schedules, all else being equal, by allowing younger and older individuals not to work (Appendix B). Production schedules do not affect relationships (12) or (13). The major effect of a shift in the age pattern of production is a large change in $Y(0)$, and in fact this single parameter shift is almost entirely responsible for the decrease in $\hat{E}$ for a given Y in the center panel of Fig. 2. The reason for this change is straightforward: higher environmental productivity is needed to meet the population's needs if individuals spend less time working, and in fact $Y(0)$ for the short work schedule, with all other parameters at favorable values, is approximately double that of the favorable-case $Y(0)$. Consequently, with yields constant at the long-schedule $Y(0)$, shortening the work schedule reduces equilibrium life expectancy by about 6–9 years. Thus, yield and labor affect growth rate and well-being similarly, and are interchangeable to some degree: if yield is high enough, populations can afford to work less, and conversely, populations can offset low yields to the extent to which more individuals are available to work.

Fig. 3 shows the effects of changing the maximum life expectancy and survival elasticities, such as might occur through a change in climate. Solid lines show the favorable case as in Fig. 2. Dashed lines show $e_0(0)$ changed to a low value (Appendix B) with all other parameters equal to their favorable-case values, while dotted lines show survival elasticities α_x changed to double their empirical value, all else being equal. The top panel shows shifts in the scaled growth rate $\hat{\lambda}_1/\lambda_1(0)$ as a function of $\hat{E}$. The bottom panel shows the unscaled growth rate $\hat{\lambda}_1$ as a function of Y. The effect of yield is very similar in the two different cases, but with two different maxima $\lambda_1(0)$. When $e_0(0)$ is lower, $Y(0)$ is also lower, resulting in a slightly larger $\hat{E}$ for a given value of Y that compensates somewhat for the steeper slope of $\hat{\lambda}_1/\lambda_1(0)$ shown at the top. This increase in $\hat{E}$ also slightly raises equilibrium TFR for a given Y (not shown). Equilibrium life expectancy as predicted from Eq. (16) qualitatively resembles the plot of $\hat{\lambda}_1$ as a function of Y, but on the scale of maximum life expectancy rather than maximum growth rate (figure not shown). Increasing survival elasticities also slightly increases $\hat{E}$ as a function of yield, but this parameter change operates through relationship (12) rather than through $Y(0)$. The opposing effects on $\hat{E}$ and $\hat{\lambda}_1$ of changes in both maximal survival rates and maximal survival elasticities are in agreement with our graphical findings above, and are in contrast to the tandem effects of changes in Y and ϕ_x.

Fig. 4 explores the effects of fertility control, whether control occurs through reduction of maximum TFR or through an increase in fertility elasticities. Plots of Eqs. (12) and (13) are qualitatively

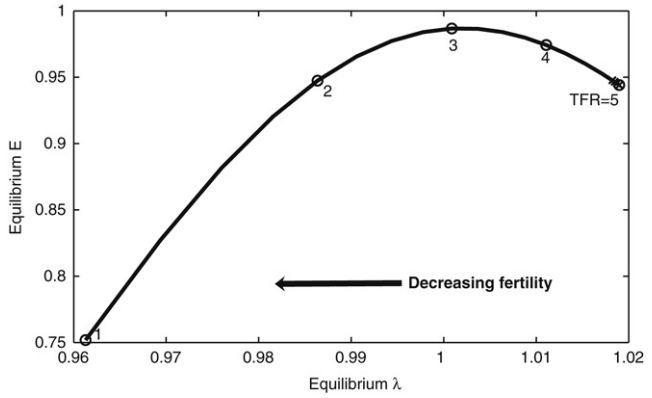

Fig. 4. Effects of fertility control on equilibrium growth rate $\hat{\lambda}_1$ and equilibrium food ratio $\hat{E}$. The solid line shows results from approximation equations (12) and (13) for varying levels of baseline TFR. Open circles show maximal TFR = 5 (no fertility control) and successively increasing control (maximal TFR = 4, 3, and 2) for reference. Maximal life expectancy is 45 and the work schedule is short. Four crosses (very close together near TFR = 5) show effects of elasticities at $\log E = 0$ at empirical levels and doubled, tripled, and quadrupled. Relative yield (Y/Y_0) is 0.94.

similar to Fig. 3; in Fig. 4 we show equilibrium pairs of $(\hat{\lambda}_1, \hat{E})$ points for different levels of fertility control. Points corresponding to baseline TFR = 5 (no control), 4, 3, 2, and 1 child per mother appear for reference. We can see that fertility control always decreases $\hat{\lambda}_1$, largely because of reductions in $\lambda_1(0)$. More importantly, the effect on $\hat{E}$ depends on the magnitude of fertility control. Control that does not reduce $\hat{\lambda}_1$ below 1 increases the equilibrium food ratio, while control that causes the population to shrink can decrease $\hat{E}$. The approximation accurately reproduces the qualitative behavior of numerical solutions to (8) and (10) . For the cases shown here, the error in the growth rate is 1% or less, while the error in the food ratio is 3% or less. Fig. 4 also shows that changes only in fertility elasticities have a much smaller effect on both $\hat{\lambda}_1$ and $\hat{E}$. This is in part because the yield used in Fig. 4 is relatively high, with $Y/Y(0) = 0.94$. A lower yield results in greater effects of changing elasticities on both $\hat{\lambda}_1$ and $\hat{E}$. The qualitative effects, however, are the same as with higher yields: increasing fertility elasticities by a factor of up to 4 decreases the growth rate but increases the food ratio.

We have seen that the impact of a given factor on $\hat{E}$ and its associated measures of well-being may or may not be the same as its effect on $\hat{\lambda}$, depending on which model parameters express the change. Thus, different aspects of environmental quality and the decisions people make with respect to labor investment and fertility can have far-reaching consequences for the well-being of individuals and for the long-run relationship between a society and its natural environment.

4. Local stability and demographic cycles

The equilibrium of the previous section is biologically and socially relevant only if it is dynamically stable. Our model's simple equilibrium of geometric growth may tempt the reader to conclude that, just as in food-independent demography, the equilibrium is always locally stable. We find, however, that this is not always the case. Following standard practice, we evaluate the stability of equilibrium using the dynamics of the perturbation equation

$$\mathbf{H}(t+1) = \mathbf{S}\mathbf{H}(t), \tag{19}$$

where $\mathbf{H}(t)$ is a perturbation to the age structure $\hat{\mathbf{u}}_t$, and we show in Appendix C that

$$\mathbf{S} = \frac{1}{\hat{\lambda}_1}\left(\mathbf{I} - \hat{\mathbf{u}}_\mathbf{1}\mathbf{e}^T\right)\left[\mathbf{A} + \mathcal{A}\hat{\mathbf{u}}_\mathbf{1}\mathbf{b}^T\right]. \tag{20}$$

Here, we write $\hat{\mathbf{A}} = \mathbf{A}(\hat{E})$,

$$\mathcal{A} = \left(\frac{\partial \mathbf{A}}{\partial \log E}\right)_{\hat{E}}, \tag{21}$$

$$\mathbf{b} = \left\{\frac{\phi(x)}{\langle \boldsymbol{\phi}, \hat{\mathbf{u}}_\mathbf{1}\rangle} - \frac{\rho(x)}{\langle \boldsymbol{\rho}, \hat{\mathbf{u}}_\mathbf{1}\rangle}\right\}, \tag{22}$$

e is a vector of ones, and superscript T indicates a transpose.

The necessary and sufficient condition for the local stability of the equilibrium is that the dominant eigenvalue of **S** be less than 1 in magnitude. We scale the equilibrium projection matrix $\hat{\mathbf{A}}$ and all its eigenvalues by its dominant eigenvalue, $\hat{\lambda}_1$:

$$\boldsymbol{A} = \frac{\hat{\mathbf{A}}}{\hat{\lambda}_1}; \quad \varrho_i = \frac{\hat{\lambda}_i}{\hat{\lambda}_1}; \quad |\varrho_i| \le 1. \tag{23}$$

This scaling does not change the eigenvectors $\hat{\mathbf{v}}_i$, $\hat{\mathbf{u}}_i$ of $\hat{\mathbf{A}}$. Then perturbation theory (see, e.g., Wilkinson (1965)) yields the approximation

$$\lambda_1(\mathbf{S}) \approx \varrho_2 + \frac{\frac{1}{\hat{\lambda}_1}\hat{\mathbf{v}}_2^\dagger \mathcal{A}\hat{\mathbf{u}}_\mathbf{1}\mathbf{b}^T\hat{\mathbf{u}}_\mathbf{2}}{\hat{\mathbf{v}}_2^\dagger\hat{\mathbf{u}}_\mathbf{2}}, \tag{24}$$

where the dagger denotes a complex conjugate transpose.

The magnitude $|\varrho_2|$ of the first term above is less than 1 because $|\hat{\lambda}_2| < \hat{\lambda}_1$. Its closeness to 1 depends on the structure of the equilibrium projection matrix: if the projection matrix were fixed at its equilibrium value, the population structure would converge to the stable structure rapidly or slowly as $|\varrho_2|$ were small or large. The second term in (24) captures the nonlinear effects of age structure on stability. When its magnitude is large enough, the dominant eigenvalue of the stability matrix exceeds 1.

We consider the magnitude of the numerator of the second term in (24) in two parts. The first, $|\mathbf{b}^T\hat{\mathbf{u}}_\mathbf{2}|$, converts the dominant component of perturbations to the stable age structure into relative excesses or deficits of food. The second, $|\hat{\mathbf{v}}_2^\dagger\mathcal{A}\hat{\mathbf{u}}_\mathbf{1}|$, measures the effects of perturbations to food supply on future demography. The product $\mathcal{A}\hat{\mathbf{u}}_\mathbf{1}$ is essentially a vector of vital-rate elasticities to food, weighted by the expected proportion of the population experiencing each rate. By elementwise multiplication of this vector with $\hat{\mathbf{v}}_\mathbf{2}$, the dominant component of perturbations to the reproductive value, we effectively select those weighted elasticities which are most important to the population's future, so that the magnitude of their sum measures food excess or deficit in demographic terms. Finally, the quantities $|\frac{1}{\hat{\lambda}_1}|$ and $|\hat{\mathbf{v}}_2^\dagger\hat{\mathbf{u}}_2|$ are scaling terms.

For human populations that successfully colonize new habitats, growth rates slightly above 1 are likely in the long run (Tuljapurkar et al., 2007), and the corresponding vital-rate elasticities are small (see Appendix B). Eq. (21) shows that the elements of the matrix $\mathcal{A}$ are directly proportional to these elasticities, so we expect the second term in Eq. (24) to be small unless perturbations are somehow amplified by changing age structure. For equilibrium growth rates near 1, numerical analysis of (24) confirms that the equilibria are stable. However, when the equilibrium growth rate and food ratio are low, the elasticities of vital rates are higher and in addition the age structure of the terms in (24) is skewed towards older ages. In such cases, a perturbation in age structure, say a drop in the number of infants, generates a strong response of the food ratio, an increase in fertility, and a large birth cohort. This large cohort in turn depresses the food ratio and drives down the size of the subsequent cohorts. In this way the feedback between age structure and hunger can drive sustained cycles. We have verified this by simulation: lowering yield and baseline survival and fertility rates, increasing vital rate elasticities, and

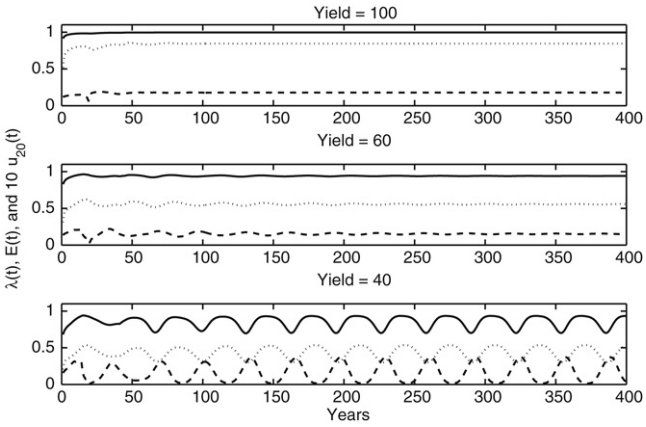

Fig. 5. Decreasing yield leads to cycles in the yearly growth rate $\lambda(t)$ (solid lines), the yearly food ratio $E(t)$ (dotted lines), and the age structure (dashed lines show ten times the proportion of 20-year-olds, $10u_{20}(t)$). Here, maximum life expectancy is low and work schedules are short; maximum TFR and mortality and fertility elasticities are empirically determined (see Appendix B). The lag between the dashed line and the two other lines represents the time between increases in the birth cohort and increases in 20-year-olds.

shortening work schedules cause all of $\lambda(t)$, $E(t)$, and $\mathbf{u}(t)$ to pass from approach to a stable point, through damped oscillations, to apparently sustained cycles at very low growth rates (Fig. 5).

We argue that sustained shocks to a population's food supply or perturbations to its age structure, such as could result from prolonged drought, epidemic, or war, could destabilize the population's dynamics. In that case, endogenous demographic cycles could make it more difficult for the population to recover. We speculate that such an interaction between environmental conditions and intrinsic demographic dynamics could have contributed to some prominent cases of rapid population decline, such as may have occurred in the American Southwest, the Pacific island of Rapa Nui, or elsewhere throughout prehistory.

5. Conclusion

The model we present here is a versatile quantitative tool that enables us to analyze how human decisions and the environment jointly determine the fates of expanding agricultural populations. It explicitly describes how food production and consumption vary by age, and articulates the relationship between food availability and vital rates in ways that separate effects of the environment from effects of society, technology, and conscious choices. We can therefore use estimates of agricultural yield in different locations to predict relative population performance. This analysis is relevant to the colonization of completely new regions, such as the different islands of Polynesia, as well as population expansion onto new, presumably more marginal agricultural lands. Due to the quantitative detail of the model, we can use agricultural yield not just to estimate a notional "carrying capacity" based on maximum production (see, e.g., several examples in Kirch (2007), but also to describe population growth, structure, and well-being. We can also apply changing environmental or social conditions to evaluate their effects on a population's trajectory through time.

An important conclusion from our work is that human choices and the environment interact to shape the state of populations. The environment can have distinct effects depending on the specific variables upon which it acts. A population may respond to a harsh environment by increasing yield via improved agricultural methods or crops, or by increasing labor, or by controlling fertility. These choices are not equivalent, and their consequences depend on an intricate interplay between population age structure, food production, and hunger. To our knowledge, this is the first quantitative model that can be used to compare such choices in substantially informative detail. Finally, we have shown that cyclic dynamics are possible if the equilibrium population growth rate is forced to low levels. In rare but serious stretches of environmental hardship, such as prolonged drought or crop epidemic, demographic dynamics could be a potent source of instability.

This paper is the first of a series on food-dependent population dynamics. Future work will examine the effects of environmental variability and of space limitation, and will investigate in detail the consequences of these factors for the well-being of preindustrial societies. Our goal is a detailed understanding of the role of environmental quality and its temporal variability, and of human strategies for exploiting or for coping with both, in the dynamics of both expanding and circumscribed populations. In the longer view, opportunities for linking food-dependent demographic models with models of agroecosystem productivity provide promising directions for integrating the effects of environment, demography, and social dynamics, and thus for the quantitative study of human populations through prehistory, history, and perhaps even the present.

Acknowledgments

We are grateful for support from NSF Biocomplexity grant BCS-0119819, NSF Agents of Change grant HSD-0624238, and the Society in Science: The Branco Weiss Fellowship (CTL). We thank our colleagues Oliver Chadwick, Michael Graves,Tony Hartshorn, Sara Hotchkiss, Patrick Kirch, Thegn Ladefoged, Cedric Puleston, and Peter Vitousek for their valuable input, and Samuel Pavard and two anonymous reviewers for their helpful comments.

Appendix A. Quantities in equilibrium approximations

For the maximally growing population with $\log E \geq 0$ and growth rate $\lambda_1(0)$, define the net maternity function (Coale, 1972)

$$\psi_x = l_x(0)m_x(0)\lambda_1(0)^{-x}, \qquad \sum_x \psi_x = 1, \tag{25}$$

and the mean length of generation

$$T_G = \sum_x x\psi_x. \tag{26}$$

Introduce ν_G, the mean elasticity of vital rates evaluated at $\log E = 0$,

$$\nu_G = \sum_x (\beta_x(0) + \gamma_x(0))\psi_x, \tag{27}$$

T_ϕ and T_ρ, the population average ages of producing and consuming food,

$$\begin{aligned} T_\phi &= \frac{\sum_x x\phi_x l_x(0)\lambda_1(0)^{-x}}{\sum_x \phi_x l_x(0)\lambda_1(0)^{-x}}, \\ T_\rho &= \frac{\sum_x x\rho_x l_x(0)\lambda_1(0)^{-x}}{\sum_x \rho_x l_x(0)\lambda_1(0)^{-x}}. \end{aligned} \tag{28}$$

a production-weighted survival elasticity,

$$\beta_\phi = \frac{\sum_x \beta_x(0)\phi_x l_x(0)\lambda_1(0)^{-x}}{\sum_x \phi_x l_x(0)\lambda_1(0)^{-x}}, \tag{29}$$

and a consumption-weighted survival elasticity,

$$\beta_\rho = \frac{\sum_x \beta_x(0)\rho_x l_x(0)\lambda_1(0)^{-x}}{\sum_x \rho_x l_x(0)\lambda_1(0)^{-x}}, \tag{30}$$

all for the maximally growing population. Then by expanding Eq. (10) around $\lambda_1(0)$, $\log E = 0$ and retaining linear terms, we find $K_1 = \left(1/[1 - (\frac{\nu_G}{T_G})(T_\rho - T_\phi) - (\beta_\phi - \beta_\rho)]\right)$. We know that the quantity in square brackets is positive because the two terms being subtracted from 1 are on the order of magnitude of elasticities at $\log E = 0$, which we expect to be small (see Appendix B); therefore K_1 itself is also positive. By expanding (8), we find $K_2 = \nu_G/T_G$. K_2 is positive because all its components are positive, and it is small because elasticities are small compared to ages.

Our stylized elasticities and labor schedule give us

$$\nu_G/T_G = \alpha(1 + \gamma/T_G),$$
$$\beta_\phi - \beta_\rho = -\alpha(T_\rho - T_\phi), \tag{31}$$

so that the denominator of K_1 becomes

$$1 - \alpha\left(2 + \frac{\gamma}{T_G}\right)(T_\rho - T_\phi). \tag{32}$$

Typically we expect $T_G \gg 1$, and $T_\phi > T_\rho$ because the youngest individuals do not work but do consume food. With these conditions, for small α and γ, expand K_1 to find the concave relationship

$$\hat{E} \approx \left(\hat{Y}/Y(0)\right)^{[1-2\alpha(T_\phi - T_\rho)]}.$$

Neglecting the contribution to (31) of fertility elasticity (which is small due to division by T_G), we obtain (18) in the text.

Appendix B. Model parameterization for simulations

For maximal age-specific survival rates, we use model mortality schedule West from Coale and Demeny (1983) to capture the shape of the survival function, varying the overall mortality level up and down as needed. We choose low and high levels of mortality to span its plausible ranges in preindustrial agricultural societies. Low maximal survival is characterized by a life expectancy at birth of 30 years, with an expectancy at ten years of 41 years (level 5, (Coale and Demeny, 1983)); the high case has 60 and 57 years, respectively (level 17, ibid). We use a fertility schedule for Polynesian populations (MacArthur, 1968), and vary the level of the schedule without changing its shape by varying the maximal TFR. The base maximum TFR is 5.0. The three maximal survival rates, together with maximal fertility of 5, result in maximal growth rates of $\lambda = 1.006$, 1.020, and 1.027, respectively. These growth rates represent a reasonable range around the 0.5% rate observed for Hawai'i and for preindustrial populations in general (Tuljapurkar et al., 2007).

The FAO and WHO (1973) provide data on human caloric needs as a function of age, and because this schedule of food requirements is based on human physiology, we do not vary it here. The FAO/WHO data do assume given activity levels, but will do for a starting point. Given these numbers, $J = 2785$ Kcal. Meanwhile, the schedule of labor as a function of age varies between societies and possibly over space and through time as well. We choose a rectangular function to describe labor, so that $\phi_x = 0$ below the age of starting work and above the age of stopping work; in between those ages, $\phi_x = 1$. This shape is a reasonable approximation to empirical schedules (e.g., Robson and Kaplan, 2003). We divide this function by two to approximate the dynamics of a society where only one sex carries out agricultural work. We examine two schedules within this framework to bracket a reasonable range of possibilities: a long work scenario, where work begins at age 10 and stops at age 65, and a short work scenario, where work begins at age 20 and stops at age 45.

We calculate age-specific survival elasticities from Bengtsson et al. (2004), and fertility elasticities from Lee (1987). Following Lee (personal communication), we average elasticity data over many locations to capture broad effects. Finally, we convert the reported elasticities of mortality to elasticities of survival, $\alpha_x(0)$. This conversion associates high maximal survival probabilities with low elasticities and low probabilities with high elasticities, so that the numerical changes in maximal survival rates reported in the text entrain changes in the survival elasticities. For the functions $p_x(E)$ and $m_x(E)$ we find it convenient to approximate the piecewise functions described in the body of the text by continuous functions. As a result of this approximation, if $\gamma_x(0)$, $\beta_x(0) > 0$, then $p_x(\log E = 0) < p_x(0)$ and $m_x(\log E = 0) < m_x(0)$, and therefore maximal vital rates do not apply precisely at $E = 1$. For the numerical results presented in this paper, we let $p_x(E)$ and $m_x(E)$ be gamma CDFs, fitting the shape parameter to the elasticity data and using a common scale parameter (set at 0.1) to give values $p_x(0)$ and $m_x(0)$ reasonably close to $p_x(0)$ and $m_x(0)$ at $\log E = 0$. These choices result in steeply S-shaped functions, which we feel are biologically plausible: since we know that survival and fertility are 0 when $E = 0$, maximal elasticities that are much less than 1 at $\log E = 0$ require a steep fall in vital rates somewhere below $E = 0$. To explore changes in the functional form, we vary both fertility and survival elasticities. Increasing the elasticities at $\log E = 0$ results in more gently sloping S-shaped functions, which are further below maximal rates at $\log E = 0$.

H, the number of person-hours worked per year, and k, the area worked in H hours, are constants that multiply the yield per unit area per year, so the effect of changing either H or α will be equivalent to varying the environmental parameter, Y. We therefore do not vary them independently. We take $Hk = 2.33$ acres/person/day from accounts of traditional Hawaiian sweet potato farming (Kamakau, 1976).

Appendix C. Derivation of the response of e_0

We consider the second term of text Eq. (16) in the special case when $\beta_x = \alpha x$. This means that the second term on the right-hand side of that equation contains $\sum_x x l_x(0)$. It is simplest to evaluate this using continuous ages as an integral,

$$\int_0^\infty dx x l_0(x).$$

Note that $(d/dx)x^2 l_0(x) = 2x l_0(x) + x^2(d/dx)l_0(x)$. Integrate both sides of this expression with respect to x, noting that $l_0(x) \to 0$ as x increases, and that $(d/dx)l_0(x) = -\mu(x)l_0(x)$ where $\mu(x)$ is the mortality rate at age x. Now $\mu(x)l_0(x)dx$ is the probability that a newborn dies between ages x and $x + dx$, so

$$\int_0^\infty dx x^2 \mu(x) l_0(x)$$

is the second moment of the age at death. Recall that e_0 is the mean age at death and let S^2 be the variance in age at death, so that the second moment equals $(e_0^2 + S^2)$. The result of the earlier integration tells us that $\int_0^\infty dx x l_0(x) = (1/2) * (e_0^2 + S^2)$.

Appendix D. Derivation of the stability equation

Consider what happens when we change the population away from equilibrium by a small vector which we write as

$$\mathbf{u}(t) = \hat{\mathbf{u}}_\mathbf{1} + \mathbf{H}(t). \tag{33}$$

Then the change in $\log \hat{E}$ is

$$\Delta \log \hat{E} = \Delta \log \hat{W} = \langle \mathbf{b}, \mathbf{H}(t) \rangle$$
$$= \Sigma\left(\frac{\phi(x)}{\langle \boldsymbol{\phi}, \hat{\mathbf{u}}_\mathbf{1} \rangle} - \frac{\rho(x)}{\langle \boldsymbol{\rho}, \hat{\mathbf{u}}_\mathbf{1} \rangle}\right) H(x, t). \tag{34}$$

Note that

$$\langle \mathbf{b}, \hat{\mathbf{u}}_\mathbf{1} \rangle = 0, \tag{35}$$

so that if we were to increase the population size by a small amount proportional to $\hat{\mathbf{u}}_\mathbf{1}$, there would be no change in $\log \hat{E}$.

The dynamics of the perturbation follow Eq. (6), which we can rewrite as

$$\mathbf{u}(t+1) = \frac{\mathbf{A}(\mathbf{E}(t))}{\lambda(t)}\mathbf{u}(t), \tag{36}$$

where

$$\lambda(t) = N(t+1)/N(t) = |\mathbf{A}(E(t))\mathbf{u}(t)|. \tag{37}$$

The matrix $\mathbf{A}(t) = \mathbf{A}(\log E(t))$ changes to

$$\mathbf{A}(t) = \hat{\mathbf{A}} + \mathcal{A}\langle \mathbf{H}(t), \mathbf{b}\rangle, \tag{38}$$

while $\lambda(t)$ changes to

$$\begin{aligned}\lambda(t) &= \left|\left(\hat{\mathbf{A}} + \mathcal{A}\langle \mathbf{H}(t), \mathbf{b}\rangle\right)(\hat{\mathbf{u}}_\mathbf{1} + \mathbf{H}(t))\right|, \\ &= \hat{\lambda}_1 + |\mathbf{G}(t)| + O(H^2),\end{aligned} \tag{39}$$

where

$$\mathbf{G}(t) = \left[\hat{\mathbf{A}} + \mathcal{A}\hat{\mathbf{u}}_\mathbf{1}\mathbf{b}^T\right]\mathbf{H}(t). \tag{40}$$

Inserting Eq. (38) and Eq. (39) into (36), expanding to linear order in H, and simplifying leads to

$$\hat{\mathbf{u}}_\mathbf{1} + \mathbf{H}(t+1) = \hat{\mathbf{u}}_\mathbf{1} + \frac{1}{\hat{\lambda}_1}\left(\mathbf{I} - \mathbf{u}_\mathbf{1}\mathbf{e}^T\right)\mathbf{G}, \tag{41}$$

which yields Eq. (20). Since $\mathbf{b}^T\hat{\mathbf{u}}_\mathbf{1} = 0$,

$$\mathbf{S}\hat{\mathbf{u}}_\mathbf{1} = 0. \tag{42}$$

Therefore, the matrix $\mathbf{S}$ has a null subspace along $\hat{\mathbf{u}}_\mathbf{1}$, and perturbations in this one-dimensional space grow at rate 0. This observation is useful in deriving the perturbation expression (24).

References

Bengtsson, T., Campbell, C., Lee, J., et al., 2004. Life Under Pressure: Mortality and Living Standards in Europe and Asia. MIT Press, Cambridge, MA, pp. 1700–1900.

Butzer, K., 1996. Ecology in the long view: Settlement, agrosystem strategies, and ecological performance. Journal of Field Archaeology 23, 141–150.

Butzer, K., 1982. Archaeology as Human Ecology: Method and Theory for a Contextual Approach. Cambridge University Press, Cambridge.

Caswell, H., 2008. Perturbation analysis of nonlinear matrix population models. Demographic Research 18, 27–83.

Chu, C.Y., Lee, R., 2006. The co-evolution of intergenerational transfers and longevity: An optimal life history approach. Theoretical Population Biology 69 (2), 193–201.

Coale, A.J., 1972. The Growth and Structure of Human Populations: A Mathematical Investigation. Princeton University Press, Princeton.

Coale, A.J., Demeny, P.G., 1983. Regional Model Life Tables and Stable Populations, 2nd ed. Academic Press, San Diego.

Durham, W., 1991. Coevolution: Genes, Culture, and Human Diversity. Stanford University Press, Palo Alto.

Durham, W., 1976. The adaptive significance of cultural behavior. Human Ecology 4, 89–121.

Edwards, R.D., Tuljapurkar, S., 2005. Inequality in life spans and a new perspective on mortality convergence across industrialized countries. Population and Development Review 31 (4), 645–675.

Joint FAO/WHO Ad Hoc Expert Committee,, 1973. Energy and Protein Requirements, Wld Hlth Org. techn. Rep. Ser., No. 522.

Kamakau, S., 1976. The Works of the People of Old. Bernice Pauahi Bishop Museum, Honolulu.

Keyfitz, N., 1968. Introduction to the Mathematics of Population. Addison-Wesley, Reading, MA.

Kirch, P.V., 1980. The archaeological study of adaptation: Theoretical and methodological issues. In: Advances in Archaeological Method and Theory, vol. 3. Academic Press, New York, pp. 101–156.

Kirch, P.V., Rallu, J.-L. (Eds.), 2007. The Growth, Regulation, and Collapse of Island Societies: Archaeological and Demographic Perspectives from the Pacific. University of Hawaii Press, Honolulu.

Lee, C.T., Tuljapurkar, S., Vitousek, P., 2006. Risky business: Spatial and temporal variation in preindustrial dryland agriculture. Human Ecology 34 (6), 739–763.

Lee, R.D., 1986. Malthus and Boserup: A dynamic synthesis. In: Coleman, D., Schofield, R. (Eds.), The State of Population Theory. Basil Blackwell, pp. 96–130.

Lee, R.D., 1987. Population Dynamics of Humans and Other Animals, Presidential Address to the Population Association of America. Demography 24, 443–466.

Lee, R.D., 1993. Accidental and Systematic Change in Population History: Homeostasis in a Stochastic Setting. Explorations in Economic History 30, 1–30.

Lee, R., 1994. The formal demography of population aging, transfers, and the economic life cycle. In: Martin, L., Preston, S. (Eds.), The Demography of Aging. National Academy Press, pp. 8–49.

Lee, R.D., 2003. Rethinking the evolutionary theory of aging: Transfers, not births, shape senescence in social species. Proc. Natl. Acad. Sci. USA 100, 9637–9642.

MacArthur, N., 1968. Island Populations of the Pacific. Australian National University Press, Canberra.

McGlade, J., 1995. Archaeology and the ecodynamics of human modified landscapes. Antiquity 69, 113–132.

Robson, A., Kaplan, H., 2003. The evolution of human life expectancy and intelligence in hunter-gatherer economies. American Economic Review 93 (1), 150–169.

Tuljapurkar, S., Lee, C.T., Figgs, M., 2007. The growth and collapse of pacific island societies. In: Vinton Kirch, P., Rallu, J.-L. (Eds.), Archaeological and Demographic Perspectives. University of Hawaii Press.

van der Leeuw, S. (Ed.), 1998. Understanding the Natural and Anthropogenic Causes of Land Degradation and Desertifiction in the Mediterranean Basin. Office for Official Publications of the European Communities, Luxembourg.

van der Leeuw, S., McGlade, J. (Eds.), 1997. Time, Process and Structured Transformation in Archaeology. Routledge, London.

van der Leeuw, S., Redman, C.L., 2002. Placing archaeology at the center of socio-natural studies. American Antiquity 67, 597–605.

Wilkinson, J.H., 1965. The Algebraic Eigenvalue Problem. Clarendon Press, Oxford.

Wood, J.W., 1998. A theory of preindustrial population dynamics — Demography, economy, and well-being in Malthusian systems. Current Anthropology 39 (1), 99–135.